Relativistic effects on the hexafluorides of group 10 metals

Jorge David [a,*], Patricio Fuentealba [b], Albeiro Restrepo [c]

[a] Departamento de Química, Universidad Andrés Bello, Republica 275, Santiago, Chile
[b] Departamento de Física, Facultad de Ciencias, Universidad de Chile, Casilla 653, Santiago, Chile
[c] Grupo de Química-Física Teórica, Instituto de Química, Universidad de Antioquia, AA 1226, Medellín, Colombia

A B S T R A C T

We present relativistic and non-relativistic *ab initio* treatments of the hexafluorides of group 10 metals. Non-relativistic equilibrium geometries belong to the D_{4h} point group while relativistic calculations afford O_h geometries. Relativistic effects yield singlet ground states for all complexes, the stabilization energy coming from the spin–orbit coupling. We used Time Dependent Density Functional Theory at the ZORA two component Regular Approximation to calculate the excitation spectra of the complexes. The predicted spectra correctly reproduce the experimental results. Relativistic effects in conjunction with spin–orbit coupling stabilize the O_h geometry and are important in the prediction of spectra and properties of the hexafluorides of the group 10 metals.

1. Introduction

Hexafluorides of group 10 metals exhibit $t_{2g}^4 e_g^0$ non-bonding molecular orbitals which are prone to splitting under the influence of the Jahn–Teller (JT) or the spin–orbit (SO) coupling effects. Aullón and Alvarez [1] investigated the existence of Palladium hexafluoride, realizing that at the non-relativistic B3LYP level, the PdF_6 complex is paramagnetic with a slight shortening of the axial distances of the octahedral geometry due to JT effect. In a similar system, crystal field theory predicts PtF_6 to be a good candidate for JT distortion [2,3]. Marx and Seppelt [4] suggested that the distortions from the O_h geometry in PtF_6 are consistent with a second order Jahn–Teller effect (SOJT), arising from the mixing of a t_{1u} orbital from the ligand with a t_{2g} orbital from the metal. Other non-relativistic *ab initio* and DFT calculations predict a D_{4h} structure [5]. It has been reported that the high electronegativity of Fluorine atoms has a magnifying effect on the relativistic properties when bonded to heavy atoms [6].

A triplet, octahedral $(5dt_{2g})^4$ geometry for PtF_6 was predicted by Wesendrup and Schwerdtfeger [7] using scalar relativistic DFT and Coupled Clusters methods. Experimental gas phase and crystalline characterizations of the PtF_6 molecule afforded structures belonging to the O_h point group [8,9]. Spectroscopy experiments support the O_h symmetry [10–12]. Absorption spectra for metal hexafluorides, including PtF_6 were measured by Moffitt and co-workers [13], their experimental results offer support for the pairing of the nd^4 electrons of the heavy ions in the group 10 hexafluorides. A non-relativistic analysis of the energy spectrum and of the distribution of electronic states [14], suggest that the triplet t_{2g} state splits to generate a singlet state, the splitting carries a reduction of the symmetry from O_h to D_{4h}. Fig. 1 gives an account of the state of affairs regarding the geometries and splittings of the MF_6 systems, including our own results to be discussed below.

The mechanism for the stabilization of the highly symmetric O_h hexafluorides of group 10 metals is not well understood. The conflicting results in relativistic vs. non-relativistic treatments of the title hexafluorides make them good subjects to study the complications that arise when the JT and SO effects are competitive. Such complexes are ideal for the study of the influence of relativity on the molecular and electronic structures and on the molecular properties determined by the electron configuration of the metal atom. In this work, we investigate the importance of relativistic effects on the stabilization of the geometries and on the molecular properties of group 10 hexafluorides.

2. Theory

When dealing with molecules containing heavy atoms, it is a well known fact that relativity has to be considered in order to obtain an accurate description of molecular properties. Within the relativistic framework, the electronic structure of a molecule is described by the approximate relativistic Dirac–Coulomb Hamiltonian, which for n-electron molecular systems containing N nuclei, under the Born–Oppenheimer approximation is usually taken to be (in atomic units)

$$H_{DC} = \sum_{i=1}^{n} h_D(i) + \sum_{i<j}^{n} \frac{1}{r_{ij}} \tag{1}$$

where $h_D(i)$ is the one body part

* Corresponding author.
E-mail addresses: j.david@uandresbello.edu (J. David), pfuente@abello.dic.uchile.cl (P. Fuentealba), albeiro@matematicas.udea.edu.co (A. Restrepo).

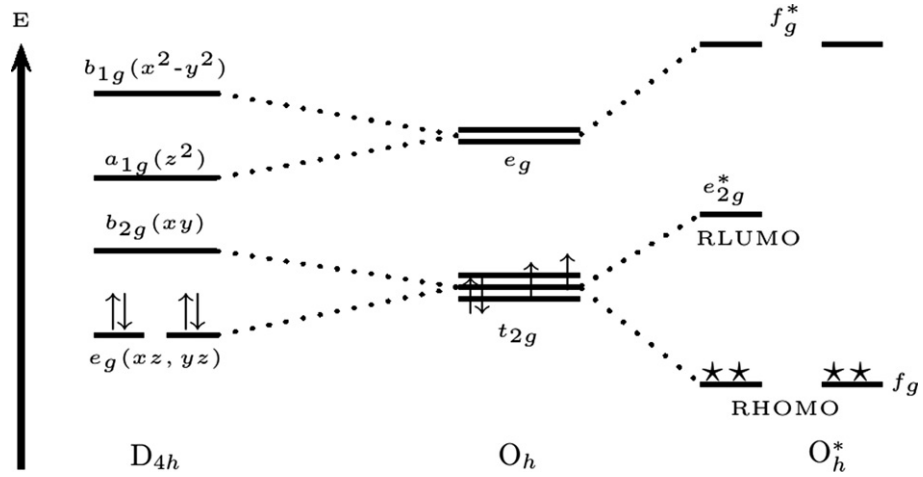

Fig. 1. Effect of relativity on the geometries and orbital splittings for the MF_6 series. Non-relativistic calculations predict singlet e_g^4, D_{4h} geometries; Crystal Field Theory predicts triplet t_{2g}^4, O_h geometries; our four component relativistic calculations predict singlet f_g^4, O_h geometries.

$$h_D(i) = c\boldsymbol{\alpha}_i \cdot \mathbf{p}_i + (\boldsymbol{\beta}_i - 1)c^2 + v(r), \tag{2}$$

where c is the speed of light, $v(r)$ potential corresponding to the interaction between the electron and the nuclei of the molecule and $\boldsymbol{\alpha}$, $\boldsymbol{\beta}$ the Dirac matrices given by

$$\boldsymbol{\alpha} = \begin{pmatrix} \mathbf{0}_2 & \boldsymbol{\sigma} \\ \boldsymbol{\sigma} & \mathbf{0}_2 \end{pmatrix}, \qquad \boldsymbol{\beta} = \begin{pmatrix} \mathbf{I}_2 & \mathbf{0} \\ \mathbf{0} & -\mathbf{I}_2 \end{pmatrix} \tag{3}$$

in Eq. (3), $\boldsymbol{\sigma}$ are the Pauli matrices.

3. Computational details

Our calculations were performed using the 4-component relativistic Dirac–Hartee–Fock (DHF) methodology as implemented in the molecular code Dirac [15]. We used a finite nuclear size with a gaussian distribution [16,17]. The uncontracted basis sets from Faegri [18] were used for Pd, Pt and Ds atoms. Exchange and correlation effects were included via a standard non-relativistic LDA calculation. For Fluorine, we used Dunning's cc-pVTZ basis set [19] plus addition of tight s orbitals with gaussian exponents 875193.80, 130626.00 and diffuse functions 1s, 1p and 1d with 0.10500, 0.07900, 0.23750 exponents, respectively. The kinetic balance condition (Eq. (4)) was used to obtain the small relativistic components of the basis set [20–23].

$$\Phi^S = -\frac{\boldsymbol{\sigma} \cdot \mathbf{p}}{2mc}\Phi^L \tag{4}$$

It has been established [20,21] that the kinetic balance criterion only ensures that the matrix representation in the finite basis approaches the correct non-relativistic limit as c tends to infinity. Model interatomic SS-integral contribution by classical repulsion of small component atomic charges [24] was used in the optimizations. We studied excitation energies for the complexes by means of two-component Time Dependent DFT (TDDFT) calculations at the XC LDA level using the Zero Order Regular Approximation (ZORA) in conjunction with the TZ2P basis sets as implemented in the molecular code ADF [25]. All electrons were considered for the SCF calculations.

4. Results and discussion

4.1. Geometries and energies

Electronic structures for the ground states of the MF_6 complexes (M = Pd, Pt, Ds) were calculated using Dirac's theory at the Dirac-DFT level by employing the Local Density Approximation (LDA) [26].

Non-relativistic optimization of the complexes afford D_{4h} structures (axially elongated octahedrons), while relativistic calculations predict structures with O_h symmetry (regular octahedrons) due to the inclusion of spin–orbit coupling effects. Accounting for correlation via LDA results in a Pt–F bond length of 1.8508 Å in the PtF_6 complex, which is in excellent agreement with the experimental values of 1.851 ± 0.002 Å [5] and 1.850 ± 0.003 Å [27]. Table 1 lists the optimized bond lengths for every case.

In the non-relativistic case, the difference in length between the axial and equatorial M–F bonds removes their degeneracy and stabilizes the non-bonding, semioccupied t_{2g} molecular orbitals due to a strong Jahn–Teller effect [28] conducing to D_{4h} structures. In the relativistic case, our calculations predict ground states with octahedral symmetries stabilized by the spin–orbit coupling. Our results agree with several reports showing that the Jahn–Teller distortion is no longer present when the spin–orbit coupling effect is accounted for [29]. In this case, the spin–orbit couplings stabilize the degenerate non-bonding electronic t_{2g} configuration. Moffitt et al. [13] studied the lowest energy electronic states for the MF_6 molecules in the third transition series by means of classical ligand field theory, they reported a very strong ligand field with a 10Dq value of ≈30000 cm^{-1}; our Dirac–LDA calculations afford 10Dq ≈29471.7 cm^{-1} for PtF_6. For the PdF_6 and DsF_6 complexes, our calculations predict 10Dq values of 23591.9 and 34625.6 cm^{-1}, respectively.

In the double group symmetry, the spin function is determined by the extra irreducible representation e_{1g}, leading to a spin–orbit ground state afforded by the direct product

$$e_{1g} \otimes t_{2g} = f_g \oplus e_{2g} \tag{5}$$

where f_g and e_{2g} are 4-dimensional and 2-dimensional extra irreducible representations, respectively. Relativistic orbitals predicted

Table 1
Relativistic (regular octahedrons) and non-relativistic (axially elongated octahedrons) optimized bond distances (Å) for the MF_6 (M = Pd, Pt, Ds) complexes

	Non-Rel.		Rel.	
	M–F(axial)	M–F(equatorial)	DHF	Dirac-LDA
Pd	1.8610	1.7780	1.7923	1.8455
Pt	1.8940	1.8060	1.8030	1.8508
Ds	1.9916	1.9038	1.8624	1.9035

Table 2
Energy gaps (cm^{-1}) for calculated molecular orbitals

	Δ_{cf}	$\Delta_{so(f_g->e^*_{2g})}$	$\Delta_{f_g->f^*_g}$
PdF_6	23591.9	1326.4	23554.9
PtF_6	29471.7	4376.4	31710.6
DsF_6	34625.6	9782.9	40632.4

Δ_{cf}: due to the crystal field.
Δ_{so}: due to the spin–orbit coupling effect.
$\Delta_{f_g->f^*_g}$: RHOMO-RLUMO+1 gap.

Table 3
Excitation energies E(eV.) and oscillator strengths f (a.u.) for the MF_6 complexes, calculated with two-component TDDFT

	E (eV)	f	RMO → RMO transitions (%)
PdF_6	1.9299	0.0150	$7f_u \rightarrow 3e_{2g}$ (46.2%), $1e_{2u} \rightarrow 3e_{2g}$ (27.7%)
			$8f_u \rightarrow 3e_{2g}$ (17.0%)
	2.8225	0.0053	$6f_u \rightarrow 3e_{2g}$ (91.9%)
PtF_6	2.9874	0.0292	$10f_u \rightarrow 4e_{2g}$ (47.5%), $3e_{2u} \rightarrow 4e_{2g}$ (25.4%)
			$11f_u \rightarrow 4e_{2g}$ (15.2%)
	3.7467	0.0112	$9f_u \rightarrow 4e_{2g}$ (89.8%)
	6.2107	0.0116	$9e_{1u} \rightarrow 11f_g$ (35.0%), $10f_u \rightarrow 11f_g$ (42.5%)
	9.1838	0.4984	$9f_u \rightarrow 11f_g$ (44.3%), $8e_{1u} \rightarrow 11f_g$ (31.5%)
DsF_6	4.2588	0.0369	$13f_u \rightarrow 5e_{2g}$ (46.1%), $5e_{2u} \rightarrow 5e_{2g}$ (20.6%)
			$12f_u \rightarrow 5e_{2g}$ (18.2%), $14f_u \rightarrow 5e_{2g}$ (13.0%)
	4.7019	0.0207	$12f_u \rightarrow 5e_{2g}$ (81.1%)
	8.9898	0.0371	$12f_u \rightarrow 12f_g$ (60.3%), $10e_{1u} \rightarrow 13f_g$ (16.7%)
			$13f_u \rightarrow 11e_{1g}$ (10.0%)
	9.5095	0.0182	$10f_u \rightarrow 4e_{2g}$ (47.5%), $11e_{1u} \rightarrow 11e_1g$ (35.6%)
			$13f_u \rightarrow 11e_{1g}$ (32.6%), $10e_{1u} \rightarrow 13f_g$ (31.1%)
	9.9474	0.0680	$10f_u \rightarrow 4e_{2g}$ (47.5%), $12f_g \rightarrow 12e_{1u}$ (42.0%)
			$10e_{1u} \rightarrow 13f_g$ (22.5%), $12f_u \rightarrow 11e_{1g}$ (22.3%)
	10.268	0.0317	$12f_g \rightarrow 15f_g$ (97.1%)
	10.869	0.2237	$10e_{1u} \rightarrow 11e_{1g}$ (30.1%), $12f_u \rightarrow 11e_{1g}$ (25.1%)
			$10e_{1u} \rightarrow 13f_g$ (13.0%)

by our calculations are: PdF_6: $8f_g$ (HOMO), $3e_{2g}$ (LUMO) and $9f_g$ (LUMO+1); PtF_6: $10f_g$ (HOMO), $4e_{2g}$ (LUMO) and $11f_g$ (LUMO+1); DsF_6: $12f_g$ (HOMO), $5e_{2g}$ (LUMO) and $13f_g$ (LUMO+1) with energy gaps as shown in Table 2.

4.2. Optical properties

For the PtF_6 complex, Moffitt et al. [13] reported two types of absorption bands, localized between 3300 and 5500 cm^{-1} (type A) and around 32000 cm^{-1} (type B), which are assigned to weak excitations associated with forbidden transitions within the partially filled $(5d)^4$ shell. Type A bands are attributed to electronic transitions within the dt_{2g} level, called $t_{3/2}$ (quartet state) and $t_{1/2}$ (doublet state). Type B bands are attributed to transitions from the lowest dt_{2g} multiplet to the de_g level. For PtF_6, our calculations afford a spin–orbit splitting of 4376.4 cm^{-1}, which corresponds to type A bands and a type B band of 31710.6 cm^{-1}, which is deviated ≈1% from the value reported by Mottiff and coworkers. Table 3 lists the excitation energies corresponding to the dominating transitions for the absorption spectra of all the complexes. In all cases, transitions are associated with the lowest energy excited state.

UV–VIS studies reveal electronic absorption patterns and detailed assignments in terms of d-d charge transfer and intra-configuration transitions. Holloway et al. [2] reported a UV–VIS signal around 23500 cm^{-1}, while Moffitt et al.[13] place it at ≈ 25000 cm^{-1}. Our TDDFT calculations for the $10f_u$, $3e_{2u}$ and $11f_u$ transitions to the $4e_{2g}$ orbital are in excellent agreement with the reported values.

References

[1] G. Aullón, S. Alvarez, Inorg. Chem. 46 (2007) 2700.
[2] J.H. Holloway, G. Stanger, E.G. Hope, W. Levason, J.S. Odgen, J. Chem. Soc. Dalton Trans. (1988) 1341.
[3] R.G. Pearson, J. Am. Chem. Soc. 91 (1969) 4947.
[4] R. Marx, K. Seppelt, R.M. Ibberson, J. Chem. Phys. 104 (1996) 7658.
[5] A.D. Richardson, K. Hedberg, G.M. Lucier, Inorg. Chem. 39 (2000) 2787.
[6] J. David, A. Restrepo, Phys. Rev. A 76 (2007) 052511.
[7] R. Wesendrup, P. Schwerdtfeger, Inorg. Chem. 40 (2001) 3351.
[8] A.D. Richardson, K. Hedberg, G.M. Lucier, Inorg. Chem. 39 (2000) 2787.
[9] R. Glauber, V. Schomaker, Phys. Rev. 89 (1953) 667.
[10] J.H. Holloway, G. Stanger, E.G. Hope, W. Levason, J.S. Ogden, J. Chem. Soc. Dalton Trans. (1988) 1341.
[11] R. Blinc, E. Pirkmajer, J. Slivnik, I. Zupancic, J. Chem. Phys. 45 (1966) 1488.
[12] T. Drews, J. Supe, A. Hagenbach, K. Seppelt, Inorg. Chem. 45 (2006) 3782.
[13] W. Moffitt, G.L. Goodman, M. Fred, B. Weinstock, Mol. Phys. 2 (1959) 109.
[14] J.H. Holloway, G. Stanger, J. Chem. Soc. Dalton Trans. (1998) 1341.
[15] H.J. Aa, Jensen, T. Saue, L. Visscher, DIRAC, A Relativistic ab-Initio Electronic Structure Program, Release 4.0, 2004.
[16] L. Visscher, K.G. Dyall, At Data Nucl. Data 67 (1997) 207.
[17] O. Visser, P.J.C. Aerts, D. Hegarly, W.C. Nieuwpoort, Chem. Phys. Lett. 134 (1987) 34.
[18] K.G. Dyall, K. Faegri, Theor. Chim. Acta 94 (1996) 39.
[19] T.H. Dunning, J. Chem. Phys. 90 (1989) 1007.
[20] Y. Ishikawa, R. Binning, K. Sando, Chem. Phys. Lett 101 (1983) 111.
[21] Y. Ishikawa, R. Binning, K. Sando, Chem. Phys. Lett 105 (1984) 189.
[22] R.E. Stanton, S. Havriliak, J. Chem. Phys. 81 (1984) 1910.
[23] L. Visscher, O. Visser, P.J.C. Aerts, H. Merenga, W.C. Nieuwpoort, Comput. Phys. Commun. 81 (1994) 120.
[24] L. Visscher, Theor. Chem. Acc. 89 (1997) 68.
[25] Amsterdam Density Functional (ADF), 2007.01 version.
[26] W. Koch, M. Holthausen, A Chemist Guide to Density Functional Theory, second ed., Wiley, 2002.
[27] R. Marx, K. Seppelt, R.M. Ibbertson, J. Chem. Phys. 104 (1996) 7658.
[28] H.A. Jahn, E. Teller, Proc. Roy. Soc. A 161 (1937) 220.
[29] W. Domcke, S. Mishra, L.V. Poluyanov, Chem. Phys. 322 (2006) 405.